BIOCHEMISTRY
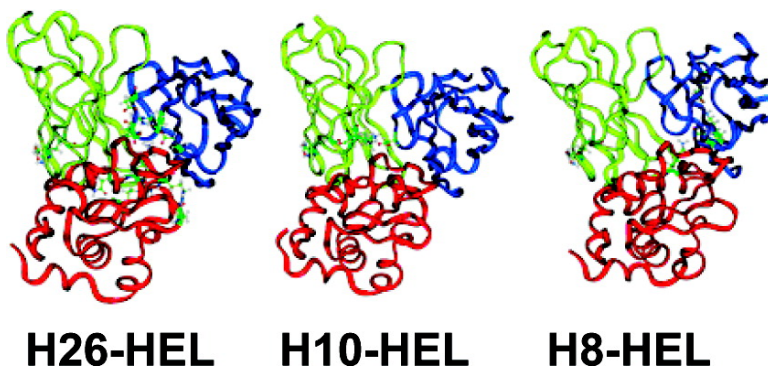### including biophysical chemistry & molecular biology

Article

Association Energetics of Cross-Reactive and Specific Antibodies

S. Mohan, Katerina Kourentzi, Kari A. Schick, Christian Uehara, Claudia A. Lipschultz,
Mauro Acchione, Morgan E. DeSantis, Sandra J. Smith-Gill, and Richard C. Willson

H26-HEL   H10-HEL   H8-HEL

More About This Article

Additional resources and features associated with this article are available within the HTML version:

- Supporting Information
- Access to high resolution figures
- Links to articles and content related to this article
- Copyright permission to reproduce figures and/or text from this article

View the Full Text HTML

ACS Publications
High quality. High impact.

Association Energetics of Cross-Reactive and Specific Antibodies[†]

S. Mohan,[‡,§] Katerina Kourentzi,[‡] Kari A. Schick,[‡,||] Christian Uehara,[‡] Claudia A. Lipschultz,[⊥] Mauro Acchione,[⊥] Morgan E. DeSantis,[⊥] Sandra J. Smith-Gill,[⊥] and Richard C. Willson*[,‡,#]

Department of Chemical and Biomolecular Engineering, University of Houston, Houston, Texas 77204-4004, Department of Biology and Biochemistry, University of Houston, Houston, Texas 77204-5001, and Structural Biophysics Laboratory, Center for Cancer Research, National Cancer Institute, Frederick, Maryland 21702-1201

Received October 9, 2008; Revised Manuscript Received December 22, 2008

ABSTRACT: HyHEL-8, HyHEL-10, and HyHEL-26 (HH8, HH10, and HH26, respectively) are murine monoclonal IgG$_1$ antibodies which share over 90% variable-region amino acid sequence identity and recognize identical structurally characterized epitopes on hen egg white lysozyme (HEL). Previous immunochemical and surface plasmon resonance-based studies have shown that these antibodies differ widely in their tolerance of mutations in the epitope. While HH8 is the most cross-reactive, HH26 is rigidified by a more extensive network of intramolecular salt links and is highly specific, with both association and dissociation rates strongly affected by epitope mutations. HH10 is of intermediate specificity, and epitope mutations produce changes primarily in the dissociation rate. Calorimetric characterization of the association energetics of these three antibodies with the native antigen HEL and with Japanese quail egg white lysozyme (JQL), a naturally occurring avian variant, shows that the energetics of interaction correlate with cross-reactivity and specificity. These results suggest that the greater cross-reactivity of HH8 may be mediated by a combination of conformational flexibility and less specific intermolecular interactions. Thermodynamic calculations suggest that upon association HH8 incurs the largest configurational entropic penalty and also the smallest loss of enthalpic driving force with variant antigen. Much smaller structural perturbations are expected in the formation of the less flexible HH26 complex, and the large loss of enthalpic driving force observed with variant antigen reflects its specificity. The observed thermodynamic parameters correlate well with the observed functional behavior of the antibodies and illustrate fundamental differences in thermodynamic characteristics between cross-reactive and specific molecular recognition.

The association of antibodies with antigens is a critical component of immune function, and the processes of recognition and association are underlying features of all protein−protein interactions. The immune system is, however, unique in the occurrence of both highly specific and nonspecific (cross-reactive and polyreactive) interactions involving different types of antibodies. An understanding of antibody−antigen association is of growing importance for engineering of antibodies for therapeutic and diagnostic applications. Several antibody−antigen complexes have been extensively characterized not only for their immunological and clinical interest but also as model systems to elucidate the general principles of protein−protein interactions (*1−3*). Antibodies recognizing hen egg white lysozyme (HEL) have often been used, with the majority of these studies addressing

molecular, thermodynamic, and kinetic features of antibodies with high specificity. There are significantly fewer reports addressing the molecular basis of recognition by cross- and polyreactive or heteroclitic antibodies.

In this work we demonstrate for the first time that the associations of cross-reactive and specific antibodies differ thermodynamically in a systematic way. HyHEL-8 (HH8) and HyHEL-26 (HH26) are high-affinity anti-HEL antibodies which recognize the same structurally characterized epitope as the HyHEL-10 (HH10) antibody (*4−8*). While HH26 is highly specific, HH8 is significantly more cross-reactive and tolerant of epitope mutations that significantly inhibit or abolish the binding of HH26. The degree of specificity or cross-reactivity of HH10 lies between that of HH8 and HH26. Previous reports on this family of antibodies by Smith-Gill et al. (*4, 5, 9−12*) have led to an understanding of some of the molecular origins of their functional differences, especially in their kinetics of association and dissociation.

Here we present a thermodynamic comparison of HH10 complex formation with HEL and the natural epitope variant Japanese quail egg white lysozyme (JQL) containing the hot spot mutation R21Q, as well as three other mutations in the epitope, with the corresponding complexes of HH8 and HH26 using isothermal titration calorimetry. The results obtained advance our understanding of the specificity of antibodies and their cross-reactivity with mutant antigens.

* Corresponding author: e-mail, Willson@uh.edu; phone, (713) 743-4308; fax, (713) 743-4323.

[‡] Department of Chemical and Biomolecular Engineering, University of Houston.

[§] Present address: Medarex, Inc., 1324 Chesapeake Terrace, Sunnyvale, CA 94089.

[||] Present address: 7413 Churchill Square, Mentor, OH 44060.

[⊥] Center for Cancer Research, National Cancer Institute.

[#] Department of Biology and Biochemistry, University of Houston.

MATERIALS AND METHODS

Antibody Production and Purification. Supernatant enriched with HH10 IgG was produced at the National Cancer Institute as previously described (*7*). The supernatants of hybridoma cell lines producing the HH8 and HH26 monoclonal antibodies (*7, 13, 14*) were produced by the National Cell Culture Center and stored at −80 °C until purification.

HH10 protein was purified by sequential anion-exchange, hydroxyapatite, and hydrophobic interaction chromatography. Anion-exchange chromatography used a Q-Sepharose Fast Flow column (diameter, 2.5 cm; length, 25 cm) (GE Healthcare). The column was equilibrated with 50 mM Tris and 0.1 mM EDTA, pH 8.0 (buffer A). After loading, the column was washed with buffer A, and protein was eluted with a gradient of NaCl in buffer A (0−400 mM; 25 column volumes). Peaks containing the antibody were identified by silver-stained 8−25% gradient SDS−PAGE gels (PhastSystem; GE Healthcare) or dot blot immunoassays, then pooled, and dialyzed in 10 mM sodium phosphate, pH 6.8, in preparation for the hydroxyapatite column. The dot blot immunoassays were based on the binding of HH10 (preincubated for 2 h with and without 1 mg/mL HEL) to HEL adsorbed on nitrocellulose membranes (Pierce). This HEL competition assay was used to distinguish between specific and nonspecific adsorption. Membranes were blocked with 3% nonfat dry milk before binding the HH10 samples, and HH10 was detected with a protein G−alkaline phosphatase conjugate (Pierce) using the BCIP/NBT (Pierce) chromogenic substrate as described by the manufacturer.

The pooled ion-exchange fractions were further purified by hydroxyapatite chromatography (Bio-Gel HT; Bio-Rad; diameter, 2.5 cm; length, 60 cm). The HH10 antibody was eluted using a gradient of sodium phosphate, pH 6.8 (10−300 mM; 5 column volumes). Fractions containing HH10 were pooled and concentrated to a final volume of ca. 20 mL using a stirred ultrafiltration cell with a YM10 membrane (Spectrum, Gardena, CA) and then dialyzed overnight in 10 mM Tris and 1 M NaCl, pH 7.0, in preparation for hydrophobic interaction chromatography.

The hydrophobic interaction adsorbent used was phenyl-Sepharose (GE Healthcare; column diameter, 2.5 cm; length, 25 cm). The isocratic eluant (10 mM Tris plus 1 M NaCl, pH 7.0) was chosen to prevent HH10 adsorption, while promoting BSA adsorption (the primary contaminant remaining after the hydroxyapatite chromatography step). Fractions containing HH10 were concentrated to ≥1 mg/mL using a stirred ultrafiltration cell (Spectrum, Gardena, CA). SDS−PAGE was used to assess purity of the final HH10 antibody preparation and showed only bands corresponding to the antibody heavy and light chains. The binding activity of the final HH10 preparation was assayed by dot blot as described previously (*15*).

HH8 and HH26 were purified using the protein A or protein A/G columns from the ImmunoPure IgG purification kit (Pierce). Purified proteins were checked for purity on silver-stained Phast SDS−PAGE gels (GE Healthcare).

Lysozyme Purification. HEL (2× crystallized) was obtained from Worthington (Freehold, NJ). Size exclusion chromatography and silver-stained SDS−PAGE were used to establish that the HEL used (lot number 32C875) was at least 99% pure and free of aggregates. HEL activity was also tested using the *Micrococcus lysodeikticus* lysis assay (*16*).

Japanese quail eggs were obtained from Stevenson Game Bird Farm (Riverside, TX) and from Truslow Farms, Inc. (Chestertown, MD); Truslow Farms was a supplier used in the earlier study of Lavoie et al. (*4*). JQL from both sources exhibited identical calorimetric results, and the results reported are those obtained using the eggs from Stevenson Game Bird Farm. Upon receipt the egg white was separated from the yolk and stored at −80 °C for later purification of lysozyme. The egg white was thawed and homogenized briefly in a Waring blender. This material was filtered through two layers of cheesecloth and then two layers of Kimwipes, diluted with six times the original egg white volume of 15 mM ammonium acetate, pH 9.2, and contacted with 10 g of CM-Sephadex (GE Healthcare) per 100 mL of egg white at 4 °C with gentle stirring. After overnight adsorption the supernatant was decanted and replaced with an equal volume of 15 mM ammonium acetate, pH 9.2, every hour until the liquid was clear (typically three times). The adsorbent was then packed into an empty 5 cm diameter chromatography column, and the adsorbed proteins (largely JQL) were eluted with 500 mM ammonium acetate, pH 9.4. This material was concentrated using an ultrafiltration cell with a YM10 membrane (Spectrum, Gardena, CA) and loaded onto a Sephacryl S-100 HR (GE Healthcare) column (diameter, 2.5 cm; length, 40 cm). Loading volume was ca. 10 mL, and the running buffer was 15 mM ammonium acetate, pH 9.2. During the purification the *M. lysodeikticus* lysis assay (*16*) was used to identify fractions containing lysozyme. Final purification was achieved using a CM-Sepharose (GE Healthcare) column (diameter, 5 cm; length, 8 cm); lysozyme was eluted with a 1.0 L gradient of ammonium acetate, pH 9.2 (15 mM−500 mM). Lysozyme was the main peak eluting during the second half of the gradient and was found to give a single band upon silver-stained SDS−PAGE analysis.

Sample Preparation for Calorimetry. Experiments were carried out in 10 mM sodium phosphate adjusted to pH 8.0 (except where noted) at the intended experimental temperature in an environmental room (NorLake Scientific, Hudson, WI). HH10 and HEL samples of ca. 5 mL each were codialyzed overnight at 4 °C against the same 4 L volume of buffer to ensure precise matching of the buffer concentration and pH. After dialysis, the concentrations of HEL and HH10 solutions were determined by absorption measurements at 280 nm using a Beckman DU-64 spectrophotometer. The extinction coefficient used for HEL was $E_{281.5} = 2.64$ (*17*), and the molecular mass used for HEL was 14388 Da (*18*). The HEL extinction coefficient was also used for JQL since the two lysozymes differ in only one absorbance-active residue (Phe 3 to Tyr), which would produce a difference in the molar extinction coefficient of less than 4% (*19*). The molecular mass of HH10 was taken as 150000 Da, and the extinction coefficient was estimated as $E_{280} = 1.43$ (K. A. Xavier, unpublished results) by the method of Gill and von Hippel (*19*) using the known HH10 Fv sequence and the constant region sequences of the murine (Balb/c) plasmacytoma MOPC-21 (*20*). HEL concentration was adjusted by the addition of dialysis buffer to a concentration that (after centrifugation as described below) would saturate all anti-

body binding sites near the midpoint of the calorimetric titration. All samples were centrifuged at $100000 \times g$ in a Beckman TL-100 ultracentrifuge for 30 min immediately before use. After centrifugation the final concentrations of antibody and lysozyme samples were determined spectrophotometrically. The A_{280} of protein samples was reduced by up to 25% after centrifugation, and they were free of any detectable scattering at wavelengths above 350 nm.

Isothermal Titration Calorimetry. An OMEGA isothermal titration calorimeter (Microcal, Northampton, MA) was used for all experiments as described previously (*15, 21*). The design and operation of the instrument have been previously described by Wiseman et al. (*22*). A voltage conditioner (Tripp Lite) and a ferroresonant transformer (General Signal) were connected in series for power stabilization, and a circulating water bath (Haake model A81) was used to stabilize the experimental temperature.

Data analysis was carried out as described previously (*15, 21*) using ORIGIN, the data analysis software provided with the calorimeter. Manual peak-by-peak integration yielded better representations of the data than did the automatic baseline determination provided by the software. The integrated areas for injections prior to saturation typically varied by less than 4% and were averaged to obtain the apparent binding enthalpy. To obtain the reported enthalpies, the apparent binding enthalpy values were corrected for the small dilution enthalpy resulting from titrating HEL into HH10/HEL complex solution. This was determined by averaging the integrated areas obtained for injections after saturation. All calorimetric titrations were repeated at least twice.

SPR Measurements. Preequilibrium rate constants for binding were determined using a Biacore 2000 (GE Healthcare Bio-Sciences, Uppsala, Sweden) instrument. Fabs refolded from *Escherichia coli* inclusion bodies (*6, 9*) were always used in order to study monovalent inherent affinities. Fab samples in HBS buffer (10 mM HEPES, 150 mM NaCl, 0.005% P20, pH 7.4) were injected over a CM5-dextran chip immobilized with different levels of amine-coupled HEL to provide surfaces that ranged from 60 response units (RUs) to 150 RUs. Previous SPR and fluorescence anisotropy studies have demonstrated that the interaction of these antibodies with HEL results in complex time-dependent two-step binding kinetics (eq 1) that are best evaluated using a series of different injection times (*10, 23*).

$$A + B \underset{k_{-1}}{\overset{k_1}{\rightleftharpoons}} AB* \underset{k_{-2}}{\overset{k_2}{\rightleftharpoons}} AB \qquad (1)$$
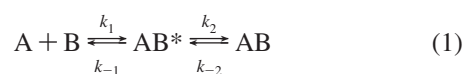
The SPR experimental protocol consisted of four analyte-inject (association) times of 10, 25, 60, and 120 min, followed by a 2 h dissociation phase with HBS buffer. Sensorgrams were corrected using a blank flow cell from the same chip that had been exposed to the same amine-coupling protocol without protein. These corrected sensorgrams were then pooled for global analysis using the two-step model in the BiaEvaluation 3.0 (eq 1). Representative SPR data and associated fits are given in the Supporting Information. $\Delta G°$ was calculated from the net binding affinity, K_A. Experiments with HH10 were performed at 10, 25, and 37 °C. Calculations using SPR measurements of ΔG and ITC estimates of ΔH and ΔC_p, with their experimental errors propagated for all calculations, showed that small differences among temperatures did not produce significant
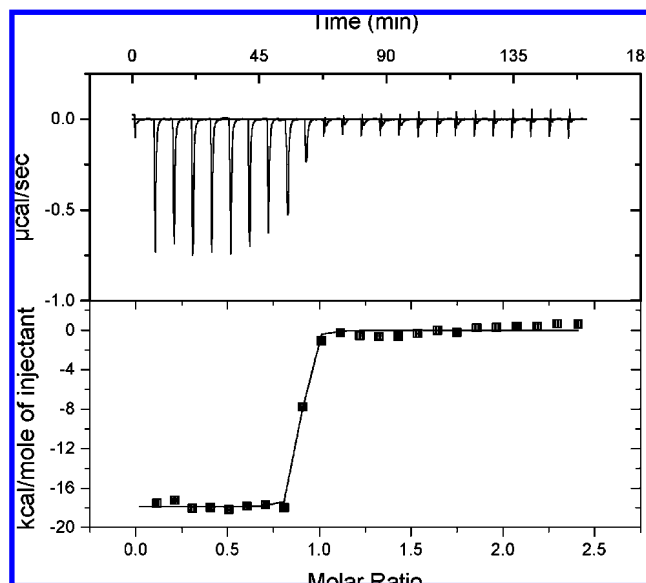

FIGURE 1: Calorimetric titration profile of association of HH8 with HEL at 25 °C.

differences among the calculated entropy values. Reliable estimates of some rate constants at the highest and lowest temperatures are extremely difficult to obtain for HH26 and HH8 associations. This is because at 37 °C very little HH26 binds to the surface, especially to JQL; k_{-1} is very high and k_2 is very low, making estimates unreliable. Similarly, at low temperatures, such as 10 °C, rates are very slow, and in the case of HH8 observed off rates may be as low as only 1 or 2 RUs during a 4 h dissociation period. Even in the case of HH10 binding to JQL, some rate constants were difficult to measure, thus accounting for relatively high error rates in the ΔG estimates for these complexes. The empirically determined values of ΔG at all three temperatures were used for HH10 complexes (the variation with temperature is very small; see Table 2). To estimate ΔG values for HH26 and HH8 complexes at 10 and 37 °C the nonlinear van't Hoff equation (eq 2) was used, using experimentally measured $\Delta G°$ at 25 °C and experimental values of ΔC_p from ITC:

$$\Delta G_T = \Delta G_0 + \Delta C_p(T - T_0) - T\Delta C_p \ln\left(\frac{T}{T_0}\right) \qquad (2)$$

where T_0 is the standard temperature, 25 °C. This approach is supported by the observation that estimating ΔG_T values for HH10 at 10 and 37 °C by the same method gave values that all were within the standard error of the observed 10 and 37 °C data (data not shown).

RESULTS

Association Energetics of HH10 with HEL and JQL. Figure 1 shows the results of the calorimetric titration of HH8 with HEL; these results are representative of the high-affinity HEL titration of all three antibodies. The top panel shows the raw titration data, and the bottom panel shows the integrated area for each injection, as a function of the molar ratio of HEL to total antibody binding sites. The high affinity of antibody/HEL association precludes the determination of affinity by calorimetric titration, as described by Wiseman et al. (*22*). Experiments were designed, therefore, to facilitate accurate measurement of the enthalpy and

Table 1: Titration Calorimetry Results for HH10 with Hen Egg Lysozyme (HEL) and Japanese Quail Egg Lysozyme (JQL)

buffer	lysozyme	temp (°C)	ΔH (kcal mol^{-1})	equivalence ratio
10 mM NaPO$_4$, pH 8.0	HEL	37.0	-24.1 ± 0.28	0.75 ± 0.05
10 mM NaPO$_4$, pH 8.0	JQL	37.0	-14.2 ± 0.20	0.92 ± 0.07
10 mM NaPO$_4$, pH 8.0	HEL	25.0	-21.1 ± 0.83	0.70 ± 0.04
10 mM NaPO$_4$, pH 8.0	JQL	25.0	-10.3 ± 0.37	0.78 ± 0.12
10 mM NaPO$_4$, pH 8.0	HEL	10.0	-17.4 ± 0.76	0.86 ± 0.02
10 mM NaPO$_4$, pH 8.0	JQL	10.0[a]	-5.8 ± 0.23	0.72 ± 0.08
10 mM Tris, pH 8.0	HEL	25.0	-20.5 ± 0.21	0.78 ± 0.01
10 mM Tris, pH 8.0	JQL	25.0	-9.8 ± 0.17	0.78 ± 0.28
10 mM NaPO$_4$, pH 8.0, + 100 mM NaCl	HEL	25.0	-19.7 ± 0.56	0.92 ± 0.01
10 mM NaPO$_4$, pH 7.0	HEL	25.0	-20.6 ± 0.28	0.72 ± 0.06

[a] Actual experimental temperature 13.5 °C; ΔH value at 10 °C extrapolated using ΔC_p. All other experimental temperatures were within 0.3° of reported temperature.

Table 2: Energetics of Association of HEL with HH8, HH10, and HH26

mAb	temp (°C)	ΔG^a (kcal mol^{-1})	ΔH (kcal mol^{-1})	ΔC_p (cal mol^{-1} K^{-1})	ΔS (cal mol^{-1} K^{-1})	$-T\Delta S$ (kcal mol^{-1})	$\Delta S_{solv}{}^b$ (cal mol^{-1} K^{-1})	$\Delta S_{conf}{}^b$ (cal mol^{-1} K^{-1})
HH8	37	-14.5	-21.3	-363.9 ± 15.1	-21.6	6.8	78.8	-92.7
	25	-14.6 ± 0.1	-17.3 ± 0.4		-9.1 ± 1.49	2.7 ± 0.4	93.2 ± 3.9	-94.3 ± 4.1
	10	-14.5	-11.5		10.5	-3.0	112.0	-93.5
HH10	37	-13.1 ± 0.2	-24.1 ± 0.3	-248.1 ± 1.0	-35.5 ± 1.2	11.0 ± 0.4	53.8 ± 0.2	-81.2 ± 1.2
	25	-13.0 ± 0.1	-21.1 ± 0.8		-27.2 ± 2.7	8.1 ± 0.8	63.6 ± 0.3	-82.7 ± 2.7
	10	-13.0 ± 0.1	-17.4 ± 0.8		-15.5 ± 2.9	4.4 ± 0.8	76.4 ± 0.3	-83.9 ± 2.9
HH26	37	-12.0	-22.2	-238.8 ± 30.3	-32.9	10.2	51.7	-76.6
	25	-12.3 ± 0.1	-18.6 ± 4.7		-21.1 ± 1.6	6.3 ± 0.5	61.2 ± 7.8	-75.0 ± 7.9
	10	-12.0	-15.7		-13.1	3.7	73.5	-78.9

[a] Experimental values (± 1 SD) at all three temperatures for HH10; for HH8 and HH26 experimental values (± 1 SD) at 25 °C and estimated values at 10 and 37 °C using the nonlinear van't Hoff equation as described in Materials and Methods. [b] $\Delta S = \Delta S_{solv} + \Delta S_{conf} + \Delta S_{crat}$; $\Delta S_{solv} = \Delta C_p \ln(T/T_s^*)$, $T_s^* = 385$ K; $\Delta S_{crat} = -8$ cal K^{-1} mol^{-1} (*43*).

stoichiometry of antibody/HEL binding and the small apparent HEL heat of dilution. Dilution-corrected heats of association for HH10/HEL association are shown in Table 1, along with the standard deviation associated with each value of ΔH.

Table 1 also presents the experimental equivalence ratio (typically 0.80), determined by dividing the number of moles of lysozyme present in the cell at the calorimetrically indicated stoichiometric equivalence by the number of moles of antibody combining sites present (*15, 21*). Deviation from unity can be attributed to the presence of inactive antibody molecules or impurities and/or inaccuracies in the antibody molecular mass or extinction coefficient used. Injection of lysozyme, for which the mass and extinction coefficients are better known, increases the precision of the energetic measurements. Table 1 lists values of HH10/HEL association enthalpies in 10 mM sodium phosphate, pH 8.0, at temperatures ranging from 10 to 37 °C. As a control for proton liberation or uptake upon binding, experiments were also performed in 10 mM Tris, pH 8.0, at 25 °C. The values of ΔH measured in Tris buffer (enthalpy of ionization, 11.51 kcal mol^{-1} at 25 °C) did not differ significantly from those measured in phosphate buffer (enthalpy of ionization, 1.22 kcal mol^{-1} at 25 °C (*24*)) showing that the contribution of buffer titration to the observed ΔH is negligible. As shown in Table 1, ΔH also does not vary significantly upon addition of 100 mM NaCl or upon changing the pH from 8.0 to 7.0.

The enthalpy of HH10/HEL association declines linearly from -17.4 kcal mol^{-1} at 10 °C to -24.1 kcal mol^{-1} at 37 °C, giving a constant value of ΔC_p of -248.1 ± 1.0 cal mol^{-1} K^{-1} (Table 2). The SPR-derived ΔG values for each temperature (Table 2) and the experimentally determined values of ΔH as a function of temperature were used to calculate ΔS values as a function of temperature. HH10/HEL association is accompanied by a favorable enthalpy change and unfavorable entropy change at all temperatures studied.

The energetics of titration of HH10, as well as HH8 and HH26, with JQL are presented in Table 3. Buffer controls for proton liberation or uptake as described above indicated that no significant proton liberation/uptake occurs upon JQL/HH10 association.

The SPR-derived ΔG values and the ITC-determined values of ΔH as a function of temperature were used to calculate values of ΔS over the temperature range of interest (Table 3). The enthalpy of HH10/JQL association declines linearly from -5.8 kcal mol^{-1} at 10.0 °C to -14.2 kcal mol^{-1} at 37.0 °C, yielding a constant ΔC_p of -310.7 ± 8.5 cal mol^{-1} K^{-1}.

Association Energetics of HH8 and HH26 with HEL and JQL. These systems were studied by the same methods as described above for HH10, though in less detail (Table 2). Stoichiometric equivalence ratios were as close or closer to unity as observed for HH10, and experimental errors were similar to those for the HH10 system (average standard error 2.5%). The affinity of HH26 for JQL was low enough to be determined calorimetrically (Figure 2); all ΔG values used to calculate the derived thermodynamic parameters in Tables 2−4 were SPR-derived/estimated. It is noteworthy that the calorimetrically determined affinity for HH26/JQL association at 25 °C is 1.32×10^{-7} M, giving a total change in free energy upon binding $\Delta G = -9.58$ kcal mol^{-1}, which compares well with the value of -8.5 kcal mol^{-1} obtained using the very different method of SPR.

DISCUSSION

Antibody Association with HEL. Association of all three antibodies with HEL is enthalpically driven with an entropic

Table 3: Energetics of Association of JQL with HH8, HH10, and HH26

mAb	temp (°C)	ΔG^a (kcal mol⁻¹)	ΔH (kcal mol⁻¹)	ΔC_p (cal mol⁻¹ K⁻¹)	ΔS (cal mol⁻¹ K⁻¹)	$-T\Delta S$ (kcal mol⁻¹)	$\Delta S_{solv}{}^b$ (cal mol⁻¹ K⁻¹)	$\Delta S_{conf}{}^b$ (cal mol⁻¹ K⁻¹)
HH8	37	−11.4	−13.3	−338.1 ± 16.4	−6.1	1.9	73.3	−70.9
	25	−11.5 ± 0.3	−9.6 ± 0.2		6.2 ± 1.3	−1.9 ± 0.4	86.6 ± 4.2	−72.0 ± 44
	10	−11.5	−4.2		25.8	−7.2	104.1	−70.3
HH10	37	−11.7 ± 1.0	−14.2 ± 0.2	−310.7 ± 8.5	−8.1 ± 3.3	2.5 ± 1.0	67.3 ± 1.9	−67.4 ± 3.8
	25	−10.9 ± 1.2	−10.3 ± 0.4		2.3 ± 3.3	−0.7 ± 1.3	79.6 ± 2.2	−69.6 ± 4.8
	10	−10.2 ± 0.7	−5.8 ± 0.2		15.5 ± 2.6	−4.4 ± 0.7	95.6 ± 2.6	−72.1 ± 3.7
HH26	37	−8.5	−10.2	−213.2 ± 15.6	−5.5	1.7	46.2	−43.7
	25	−8.5 ± 0.7	−8.0 ± 0.2		1.7 ± 2.4	−0.5 ± 0.7	54.6 ± 4.0	−44.9 ± 4.7
	10	−8.5	−4.5		14.0	−3.9	65.6	−43.4

[a] Experimental values (±1 SD) at all three temperatures for HH10; for HH8 and HH26 experimental values (±1 SD) at 25 °C and estimated values at 10 and 37 °C using the nonlinear van't Hoff equation as described in Materials and Methods. [b] $\Delta S = \Delta S_{solv} + \Delta S_{conf} + \Delta S_{crat}$; $\Delta S_{solv} = \Delta C_p \ln(T/T_s^*)$, $T_s^* = 385$ K; $\Delta S_{crat} = -8$ cal K⁻¹ mol⁻¹ (43).
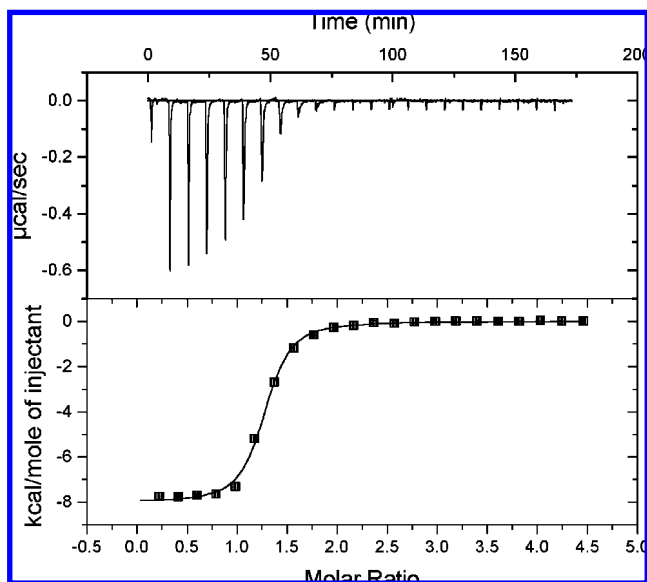

FIGURE 2: Calorimetric titration profile of association of HH26 with JQL at 25 °C.

penalty at all temperatures from 10 to 37 °C with the sole exception of H8 at 10 °C with a small favorable entropy. ΔH declines linearly with temperature; i.e., it becomes more favorable at higher temperatures. The values of ΔC_p observed are comparable to those obtained in previous studies of protein−protein associations. Calculated values of $T\Delta S$ become much less favorable as temperature increases, changing on average by 7.6 kcal mol⁻¹ over the temperature range studied, while the values of experimental and estimated SPR-derived ΔG on average change by less than 1 kcal mol⁻¹ over this range of temperatures; thus, a nearly complete enthalpy−entropy compensation occurs in this system. In all three complexes, unfavorable changes in enthalpy are compensated by reductions in unfavorable entropy as temperature decreases, typical of other antibody−antigen interactions (25−27).

We have shown elsewhere that the association kinetics of these complexes are best described by a two-step model corresponding to rapid formation of an intermediate/encounter complex, followed by a slower annealing or docking to a more stable complex (9−11, 23). We have also demonstrated that the first step of the HEL association is usually entropically driven, while the docking step is enthalpically driven with a large entropic penalty (C. A. Lipschultz et al., unpublished data).

Association of the more specific HH26−HEL complex is characterized by a higher favorable enthalpy change than HH8−HEL at all temperatures studied here, with the difference becoming more apparent at lower temperatures. The HH26−HEL interface has more hydrogen bonds, both inter- and intramolecular, and stronger electrostatic interactions than the other two complexes (6, 28). Among the HEL complexes, at each temperature studied the HH8−HEL complex has the lowest enthalpy of association, consistent with this complex having the smallest number of stabilizing hydrogen bonds and electrostatic interactions.

The entropy changes of association of the three antibodies with HEL are generally negative (unfavorable). Of the three antibody complexes with HEL, that of HH8 shows the smallest unfavorable ΔS at every temperature (Table 2). The HH8−HEL entropic change is in fact positive (favorable) at 10 °C. The change in specific heat capacity, which in part reflects the extent of burial of hydrophobic interfacial residues upon association, is larger for the HH8−HEL complex (−363.9 cal mol⁻¹ K⁻¹) than for the HH26−HEL complex (−238.8 cal mol⁻¹ K⁻¹). This is consistent with the results of structural and computational studies showing that the binding site of HH8 involves more hydrophobic residues compared to the other two antibodies (6, 28−30).

It is unusual for the interaction of an antibody with a large protein antigen to have a favorable (positive) entropy change, although associations of smaller proteins with (relatively hydrophobic) drug molecules are frequently entropically driven (31). Favorable entropy changes of association could arise in part from the contributions of the mobility of water molecules and backbone and side chain atoms in the interface, implying a lack of "tight fit" or, alternatively, an association accompanied by water exclusion and an interaction dominated by hydrophobic interactions. A fully affinity-matured antibody would be expected to show close shape complementary to its antigen, and a lack of fit would indicate either that the antibody is incompletely matured or that it has a certain degree of intrinsic cross-reactivity. A structural comparison revealed that the combining site of the chimeric HH H8L10 (heavy chain of HH8 refolded with the light chain of HH10) showed higher surface complementarity to HEL than either HH26 or HH10 (6). HH8, which is a high-affinity (higher than HH10 or HH26) antibody obtained from the hyperimmune (memory) response (7, 32), belongs to the latter category. Structural studies have shown that, during affinity maturation, somatic mutation increases the number of hydrophobic residues in the combining site at the expense

Table 4: Effect of JQL Mutations on the Association Energy Changes of HH8, HH10, and HH26 Complexes

mAb	temp (°C)	$\Delta\Delta G_{\text{JQL-HEL}}$ (kcal mol^{-1})	$\Delta\Delta H_{\text{JQL-HEL}}$ (kcal mol^{-1})	$\Delta(-T\Delta S)_{\text{JQL-HEL}}$ (kcal mol^{-1})	$\Delta\Delta S_{\text{solv}}$ (cal mol^{-1} K^{-1})	ΔS_{conf} (cal mol^{-1} K^{-1})
HH8	37	3.0	8.0	−5.0	−5.6	21.8
	25	3.0 ± 0.3	7.7 ± 0.5	−4.7 ± 0.6	−6.6 ± 5.7	22.3 ± 6.0
	10	3.0	7.3	−4.3	−7.9	23.2
HH10	37	1.4 ± 1.0	9.9 ± 0.4	−8.5 ± 1.1	13.6 ± 1.9	13.9 ± 4.0
	25	2.1 ± 1.2	10.8 ± 0.9	−8.7 ± 1.5	16.0 ± 2.2	13.2 ± 5.5
	10	2.8 ± 0.7	11.6 ± 0.8	−8.8 ± 1.1	19.3 ± 2.6	11.8 ± 4.7
HH26	37	3.5	12.0	−8.5	−5.5	32.8
	25	3.6 ± 0.7	10.6 ± 0.5	−7.0 ± 0.9	−6.6 ± 8.7	30.1 ± 9.2
	10	3.5	11.2	−7.7	−7.9	35.2

of polar residues (*6*). In addition, detailed analyses of site-directed mutants of the anti-HEL antibody D1.3 supported the hypothesis that the entropic changes in the complex were most likely related to hydrophobic interactions (*33*).

Antibody Association with JQL. The HH26−JQL complex was the only complex with affinity low enough to be reliably measured by ITC (Figure 2); the association constant calculated from ITC data agrees with that obtained by measuring the kinetics by SPR techniques. Compared to association with HEL, association of all three antibodies with JQL involves much smaller enthalpic contributions, compensated by corresponding larger favorable entropy changes. Entropic changes of association for all three complexes at 25 and 10 °C are positive. Among the three antibodies, the HH26−JQL complex has both the smallest favorable enthalpy and the largest favorable entropy of association at 37 and 25 °C, respectively. Despite this compensation, the affinity of HH26 for JQL is about 39 times lower than its affinity for HEL. HH8 shows less specificity, with an affinity for JQL only about 7 times lower than that for HEL (*5*). As in the antibody−HEL complexes, ΔC_p of the HH8−JQL complex is the largest among the three JQL complexes while that of the HH26−JQL complex is the smallest, suggesting that in the HH8−JQL complex more hydrophobic residues are involved in mediating the interaction. An overlay of the X-ray crystallographic structure of JQL (*34*), PDB code 2IHL with HEL (in the HH10−HEL complex) reveals that the conformation of the backbone of JQL around positions 101, 102, and 103 differs substantially from that of uncomplexed HEL. The C$^\alpha$ atoms of JQL, at positions 102 and 103, are shifted by 5.6 and 4.1 Å respectively, relative to their corresponding positions in HEL (*29*). JQL has the residues Val and His at positions 102 and 103 instead of the Gly and Asn respectively present in HEL. In order to accommodate the structural differences of JQL (e.g., to avoid steric clashes) the paratope of any of the antibodies would necessarily undergo some conformational changes compared to their conformations in the structures with HEL (*28*). Molecular modeling studies suggest that more extensive intramolecular salt and hydrogen bond networks would render HH10 and HH26 less likely to undergo such rearrangements than HH8 (*28, 29*).

The amino acid sequence of JQL differs from HEL in six positions, the most notable epitope change being the R21Q mutation. HEL residue Arg 21 is an epitope "hot spot" and is among the largest contributors of free energy to these complexes (*9, 13, 35, 36*). HH10 makes three hydrogen bonds with this residue and several nonbonded contacts (*8, 29, 35−38*). Mutating this arginine to glutamine, as in JQL, would lead to the loss of at least two hydrogen bonds

and several nonbonded contacts. The loss of these contacts would result in a corresponding decrease in the favorable enthalpic driving force.

Enthalpic Contributions Dominate Antibody Specificity. Previous SPR-based studies have demonstrated that epitope mutations affect the kinetics of cross-reactive and specific antibodies to varying degrees; however, the thermodynamic mechanisms that actually mediate cross-reactive or specific behavior are not understood. To investigate this issue, the mutational differences of the energetic components ($\Delta\Delta H_{\text{JQL-HEL}}$, $\Delta(-T\Delta S)_{\text{JQL-HEL}}$, and $\Delta\Delta G_{\text{JQL-HEL}}$) were calculated for the three antibodies (Table 4). The association of the highly specific HH26 with JQL compared to HEL involves both a large loss of favorable enthalpy change and a gain in favorable entropy change. The values of the corresponding changes for the association of HH8 are the smallest, and those for HH10 are intermediate.

In protein−protein associations, enthalpic change largely represents the structural composition of hydrogen bonds, electrostatic interactions, and water-mediated interactions (*31*). The specificity of an antibody is the selective recognition of its ligand through specific interactions between a select set of residues in the interacting surfaces, and hydrogen bonds and electrostatic interactions are the predominant mediators of this specificity (*31, 39, 40*). While HH10 has the largest net change in enthalpy in its association with both HEL and JQL, the mutational loss of association enthalpy, $\Delta\Delta H_{\text{JQL-HEL}}$, is generally the largest for HH26 at 37 °C, and those for both HH10 and HH26 are greater than for HH8 at all temperatures (Table 4; note the similar values for HH26 and HH10 at 25 and 10 °C; also note that the values for HH26 are within the standard error of the values for HH10 at both temperatures, Table S1). Though these losses of enthalpic driving force are partly compensated by more favorable entropy changes of association in both antibodies, there is a net reduction in affinity of HH26 for JQL of approximately 39-fold. This probably reflects the loss of some important stabilizing interactions found in both complexes and suggests that the *specificity* of the antibodies is mediated by interactions that are predominantly *enthalpic in nature*. Structure-based comparison of the numbers of geometry-sensitive hydrogen bonds, salt links, and electrostatic interactions with antigen shows that, among the three complexes, that of HH26 has the largest number of each (*6, 28, 29*) and that the contribution of intermolecular electrostatic forces is greatest in the HH26 complex (*6, 12, 28, 29*). In the modeled complexes of the three antibodies with HEL, HH26 forms 18 hydrogen bonds with HEL in comparison to the 11 hydrogen bonds formed by HH8, which correlates well with the current observation that the smallest change

in enthalpic contribution is associated with HH8. The complexes of HH10 and HH26 derive stability mainly from enthalpic energy while the smaller mutational loss of association enthalpy for HH8 (the smallest of the three) implies that this antibody is able to maintain most of the (predominantly hydrophobic) interactions (*6*) crucial for its recognition, even with mutant antigen. The magnitude of loss of enthalpic driving force for HH10 with JQL correlates with its degree of specificity, which is intermediate. These conclusions agree with those of Kumagai et al. (*41, 42*).

Configurational Entropy Mediates Antibody Cross-Reactivity. The total change in entropy ΔS is the summation of solvent, configurational, and cratic effects, represented by ΔS_{solv}, ΔS_{conf}, and ΔS_{crat}, respectively (*43*). Upon formation of the antibody−antigen complex, the variation of arrangement of water molecules around polar and apolar patches is reflected in ΔS_{solv}, while the changes in configurational freedom of backbone and side chains of both antibody and antigen are given by ΔS_{conf}. ΔS_{crat} represents the loss of translational and rotational degrees of freedom for the associating proteins and is empirically determined to be −8 cal K^{-1} mol^{-1}. ΔS_{solv} is given by $\Delta C_p \ln(T/T_s^*)$, where T_s^* is taken as 112 °C, the temperature at which the aqueous dissolution of apolar compounds is independent of the apolar surface area. The values of ΔS_{solv} and ΔS_{conf} thus calculated are listed in Tables 2 and 3 for antibody associations with HEL and JQL, respectively.

At all temperatures studied, the complexes of less specific HH8 with HEL and JQL have the largest favorable solvent contribution to entropy, as well as the largest unfavorable configurational entropic penalty to total entropic change with the sole exception of HH10−JQL at 10 °C. On the other hand, the complexes of the highly specific HH26 exhibit the smallest favorable ΔS_{solv} as well as the smallest unfavorable ΔS_{conf} at all temperatures, while the corresponding changes for HH10 lie in between (note the similar ΔS_{conf} for HEL complexes of HH10 and HH26). Since these three related antibodies are known to recognize the same structurally characterized epitope on both HEL and JQL, the differences observed in configurational entropy are probably primarily due to the structural differences among the antibody binding sites. Previous computational studies showed that the binding site of HH26 is likely to be the most rigid, because it is stabilized by the largest number of intramolecular salt bridges (*28, 29*). In contrast, the binding site of HH8 lacks these stabilizing interactions, making it the most flexible and allowing it to adopt alternate conformations (*28, 29, 44*). The binding site of HH10 has a moderate number of intramolecular salt bridges and was predicted to be of intermediate flexibility (*28, 29, 44*). The largest changes of configurational entropy (Tables 2 and 3) were seen for flexible HH8, consistent with the idea that its binding site undergoes the largest conformational rearrangement upon association. The complexes of HH8 are thus very likely formed by molecular processes most typical of induced fit associations. The conformational rearrangements in the complexes of HH8 also result in the largest buried surface area and the greatest degree of intermolecular surface complementarity (*28, 29, 44*). The increased complementarity is not necessarily due to structural rearrangements only in those segments with sequence changes in complementarity determining regions (CDR) unique to HH8 but also likely
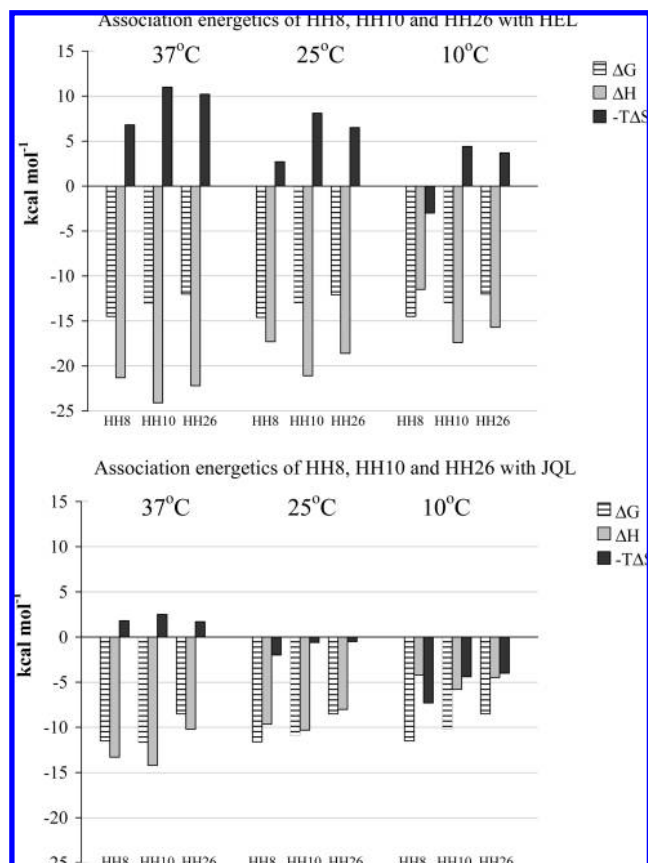

FIGURE 3: Energetics of association of HH8, HH10, and HH26 with HEL (top) and JQL (bottom).

involves subtle structural rearrangements in the other CDR's as well as in HEL. This would lead to increased complementarity both of the entire binding interface and in the areas of the interface buried upon complex formation (*41*). The intrinsic ability of HH8 to reorganize its binding site when it encounters a mutant antigen correlates with its cross-reactivity. Conformational rearrangement may also allow preservation of hydrogen bonds and electrostatic interactions that would otherwise be lost, leading to the observed smallest $\Delta\Delta H$ of antigen mutation (Table 4).

In contrast, the configurational entropic effects of HH26 complexes may reflect the lower degree of conformational rearrangement exhibited by this antibody. Structural studies comparing movements of CDR2 of the heavy chain support this hypothesis (*6*). Although this antibody has the largest overall favorable mutational $\Delta(-T\Delta S)$, this falls short of compensating for the losses of favorable ΔH. The loss of tight binding in HH26−JQL complex, evidenced by the gain in configurational freedom, is also supported by the further reduction in the already smallest estimated buried surface area. If the binding site of HH26 is unable to adopt alternate conformations that could lead to new interactions, the result would be increased configurational freedom that does not compensate for the loss of bond energy. The inability of its binding site to adopt alternate conformations, which agrees with modeling predictions and structural studies (*6, 29*), is a possible cause of its relative intolerance of epitope mutations. As the binding site of HH26 undergoes minimal structural perturbation, the association of this antibody with its antigen can be best described as a "lock and key" process.

The apparent conformational flexibility of HH8, on the other hand, helps this antibody to form new interactions by conformational rearrangement of its binding site when it encounters a mutant antigen. The higher affinity of HH8 for both HEL and variant antigens likely involves both an increase in favorable enthalpy change of association due to localized interface interactions and compensatory decreases in favorable enthalpy and unfavorable entropy due to other mutations which allow the flexibility (*41*). In addition, at any given temperature the HH8 complexes with both antigens have the highest favorable solvent portion of the entropy term compared to the respective complexes of either HH10 or HH26. This is consistent with the conclusion of Mariuzza and colleagues that hydrophobic interactions are a primary contributor to complex stability (*6, 33, 37*). The changes observed in the corresponding energetic parameters of HH10 are moderate, indicating that it is able to partially compensate for some of the lost interactions when it encounters a variant antigen by undergoing conformational rearrangement, albeit to a lesser extent than HH8.

In conclusion, here we demonstrate that the energetic bases of specific and cross-reactive association are fundamentally different. Specificity is often manifested in a preorganized combining site that mediates conserved interactions within the complex, as exhibited by HH26. While HH26 incurs only a small configurational entropic penalty in associating with the mutant antigen JQL, the inability of its rigidly precon-figured binding site to accommodate the mutant antigen precludes the formation of new interactions that could otherwise moderate its large loss of enthalpic driving force. Cross-reactivity, on the other hand, is generally associated with a more "generic", flexible binding site and less conserved interactions as evident in the association of HH8 with the mutant antigen. The binding site of HH8 probably adopts alternate conformations at the cost of large entropic penalties but forms intermolecular interactions (specific or nonspecific) that would be otherwise lost with mutant antigen.

SUPPORTING INFORMATION AVAILABLE

Representative SPR data and associated fits. This material is available free of charge via the Internet at http://pubs.acs.org.

REFERENCES

1. Lo Conte, L., Chothia, C., and Janin, J. (1999) The atomic structure of protein-protein recognition sites. *J. Mol. Biol. 285*, 2177–2198.
2. Mariuzza, R. A., Poljak, R. J., and Schwarz, F. P. (1994) The energetics of antigen-antibody binding. *Res. Immunol. 145*, 70–72.
3. Sundberg, E. J., and Mariuzza, R. A. (2002) Molecular recognition in antibody-antigen complexes. *Adv. Protein Chem. 61*, 119–160.
4. Lavoie, T. B., Drohan, W. N., and Smith-Gill, S. J. (1992) Experimental analysis by site-directed mutagenesis of somatic mutation effects on affinity and fine specificity in antibodies specific for lysozyme. *J. Immunol. 148*, 503–513.
5. Lavoie, T. B., Mohan, S., Lipschultz, C. A., Grivel, J. C., Li, Y., Mainhart, C. R., Kam-Morgan, L. N., Drohan, W. N., and Smith-Gill, S. J. (1999) Structural differences among monoclonal antibod-ies with distinct fine specificities and kinetic properties. *Mol. Immunol. 36*, 1189–1205.
6. Li, Y., Li, H., Yang, F., Smith-Gill, S. J., and Mariuzza, R. A. (2003) X-ray snapshots of the maturation of an antibody response to a protein antigen. *Nat. Struct. Biol. 10*, 482–488.
7. Newman, M. A., Mainhart, C. R., Mallett, C. P., Lavoie, T. B., and Smith-Gill, S. J. (1992) Patterns of antibody specificity during the BALB/c immune response to hen eggwhite lysozyme. *J. Immunol. 149*, 3260–3272.
8. Padlan, E. A., Silverton, E. W., Sheriff, S., Cohen, G. H., Smith-Gill, S. J., and Davies, D. R. (1989) Structure of an antibody-antigen complex: crystal structure of the HyHEL-10 Fab-lysozyme complex. *Proc. Natl. Acad. Sci. U.S.A. 86*, 5938–5942.
9. Li, Y., Lipschultz, C. A., Mohan, S., and Smith-Gill, S. J. (2001) Mutations of an epitope hot-spot residue alter rate limiting steps of antigen-antibody protein-protein associations. *Biochemistry 40*, 2011–2022.
10. Lipschultz, C. A., Li, Y., and Smith-Gill, S. (2000) Experimental design for analysis of complex kinetics using surface plasmon resonance. *Methods 20*, 310–318.
11. Lipschultz, C. A., Yee, A., Mohan, S., Li, Y., and Smith-Gill, S. J. (2002) Temperature differentially affects encounter and docking thermodynamics of antibody-antigen association. *J. Mol. Recognit. 15*, 44–52.
12. Sinha, N., and Smith-Gill, S. J. (2002) Electrostatics in protein binding and function. *Curr. Protein Pept. Sci. 3*, 601–614.
13. Smith-Gill, S. J., Lavoie, T. B., and Mainhart, C. R. (1984) Antigenic regions defined by monoclonal antibodies correspond to structural domains of avian lysozyme. *J. Immunol. 133*, 384–393.
14. Smith-Gill, S. J., and Sercarz, E. E. (1989) *The Immune Response to Structurally Defined Proteins: The Lysozyme Model*, Adenine Press, New York.
15. Hibbits, K. A., Gill, D. S., and Willson, R. C. (1994) Isothermal titration calorimetric study of the association of hen egg lysozyme and the anti-lysozyme antibody HyHEL-5. *Biochemistry 33*, 3584–3590.
16. Shugar, D. (1952) The measurement of lysozyme activity and the ultra-violet inactivation of lysozyme. *Biochim. Biophys. Acta 8*, 302–309.
17. Aune, K. C., and Tanford, C. (1969) Thermodynamics of the denaturation of lysozyme by guanidine hydrochloride. I. Depen-dence on pH at 25 degrees. *Biochemistry 8*, 4579–4585.
18. Jolles, P. (1969) Lysozymes: a chapter of molecular biology. *Angew. Chem., Int. Ed. Engl. 8*, 227–239.
19. Gill, S. C., and von Hippel, P. H. (1989) Calculation of protein extinction coefficients from amino acid sequence data. *Anal. Biochem. 182*, 319–326.
20. Kabat, E. A., Wu, T. T., Perry, H. M., Gottesman, K. S., and Foeller, C. (1991) *Sequences of Proteins of Immunoligical Interest*, 5th ed., Diane Books Publishing Co., National Institutes of Health, Bethesda, MA.
21. Xavier, K. A., and Willson, R. C. (1998) Association and dissociation kinetics of anti-hen egg lysozyme monoclonal antibod-ies HyHEL-5 and HyHEL-10. *Biophys. J. 74*, 2036–2045.
22. Wiseman, T., Williston, S., Brandts, J. F., and Lin, L. N. (1989) Rapid measurement of binding constants and heats of binding using a new titration calorimeter. *Anal. Biochem. 179*, 131–137.
23. Kourentzi, K., Srinivasan, M., Smith-Gill, S. J., and Willson, R. C. (2008) Conformational flexibility and kinetic complexity in antibody-antigen interactions. *J. Mol. Recognit. 21*, 114–121.
24. Morin, P. E., and Freire, E. (1991) Direct calorimetric analysis of the enzymatic activity of yeast cytochrome *c* oxidase. *Biochemistry 30*, 8494–8500.
25. Goldbaum, F. A., Schwarz, F. P., Eisenstein, E., Cauerhff, A., Mariuzza, R. A., and Poljak, R. J. (1996) The effect of water activity on the association constant and the enthalpy of reaction between lysozyme and the specific antibodies D1.3 and D44.1. *J. Mol. Recognit. 9*, 6–12.
26. Yokota, A., Tsumoto, K., Shiroishi, M., Kondo, H., and Kumagai, I. (2003) The role of hydrogen bonding via interfacial water molecules in antigen-antibody complexation. The HyHEL-10-HEL interaction. *J. Biol. Chem. 278*, 5410–5418.
27. Ysern, X., Fields, B. A., Bhat, T. N., Goldbaum, F. A., Dall'Acqua, W., Schwarz, F. P., Poljak, R. J., and Mariuzza, R. A. (1994) Solvent rearrangement in an antigen-antibody interface introduced by site-directed mutagenesis of the antibody combining site. *J. Mol. Biol. 238*, 496–500.
28. Sinha, N., Mohan, S., Lipschultz, C. A., and Smith-Gill, S. J. (2002) Differences in electrostatic properties at antibody-antigen binding sites: implications for specificity and cross-reactivity. *Biophys. J. 83*, 2946–2968.
29. Mohan, S., Sinha, N., and Smith-Gill, S. J. (2003) Modeling the binding sites of anti-hen egg white lysozyme antibodies HyHEL-8

and HyHEL-26: an insight into the molecular basis of antibody cross-reactivity and specificity. *Biophys. J. 85*, 3221–3236.

30. Smith-Gill, S. J., Mainhart, C., Lavoie, T. B., Feldmann, R. J., Drohan, W., and Brooks, B. R. (1987) A three-dimensional model of an anti-lysozyme antibody. *J. Mol. Biol. 194*, 713–724.

31. Todd, M. J., and Freire, E. (1999) The effect of inhibitor binding on the structural stability and cooperativity of the HIV-1 protease. *Proteins 36*, 147–156.

32. Smith-Gill, S. J., Mainhart, C. R., Lavoie, T. B., Rudikoff, S., and Potter, M. (1984) VL-VH expression by monoclonal antibodies recognizing avian lysozyme. *J. Immunol. 132*, 963–967.

33. Sundberg, E. J., Urrutia, M., Braden, B. C., Isern, J., Tsuchiya, D., Fields, B. A., Malchiodi, E. L., Tormo, J., Schwarz, F. P., and Mariuzza, R. A. (2000) Estimation of the hydrophobic effect in an antigen-antibody protein-protein interface. *Biochemistry 39*, 15375–15387.

34. Chitarra, V., Alzari, P. M., Bentley, G. A., Bhat, T. N., Eisele, J. L., Houdusse, A., Lescar, J., Souchon, H., and Poljak, R. J. (1993) Three-dimensional structure of a heteroclitic antigen-antibody cross-reaction complex. *Proc. Natl. Acad. Sci. U.S.A. 90*, 7711–7715.

35. Kam-Morgan, L. N., Smith-Gill, S. J., Taylor, M. G., Zhang, L., Wilson, A. C., and Kirsch, J. F. (1993) High-resolution mapping of the HyHEL-10 epitope of chicken lysozyme by site-directed mutagenesis. *Proc. Natl. Acad. Sci. U.S.A. 90*, 3958–3962.

36. Pons, J., Rajpal, A., and Kirsch, J. F. (1999) Energetic analysis of an antigen/antibody interface: alanine scanning mutagenesis and double mutant cycles on the HyHEL-10/lysozyme interaction. *Protein Sci. 8*, 958–968.

37. Rajpal, A., Taylor, M. G., and Kirsch, J. F. (1998) Quantitative evaluation of the chicken lysozyme epitope in the HyHEL-10 Fab complex: free energies and kinetics. *Protein Sci. 7* 1868–1874.

38. Taylor, M. G., Rajpal, A., and Kirsch, J. F. (1998) Kinetic epitope mapping of the chicken lysozyme·HyHEL-10 Fab complex: delineation of docking trajectories. *Protein Sci. 7*, 1857–1867.

39. Kwong, P. D., Doyle, M. L., Casper, D. J., Cicala, C., Leavitt, S. A., Majeed, S., Steenbeke, T. D., Venturi, M., Chaiken, I., Fung, M., Katinger, H., Parren, P. W., Robinson, J., Van Ryk, D., Wang, L., Burton, D. R., Freire, E., Wyatt, R., Sodroski, J., Hendrickson, W. A., and Arthos, J. (2002) HIV-1 evades antibody-mediated neutralization through conformational masking of receptor-binding sites. *Nature 420*, 678–682.

40. Myszka, D. G., Sweet, R. W., Hensley, P., Brigham-Burke, M., Kwong, P. D., Hendrickson, W. A., Wyatt, R., Sodroski, J., and Doyle, M. L. (2000) Energetics of the HIV gp120-CD4 binding reaction. *Proc. Natl. Acad. Sci. U.S.A. 97*, 9026–9031.

41. Kumagai, I., Nishimiya, Y., Kondo, H., and Tsumoto, K. (2003) Structural consequences of target epitope-directed functional alteration of an antibody. The case of anti-hen lysozyme antibody, HyHEL-10. *J. Biol. Chem. 278*, 24929–24936.

42. Nishimiya, Y., Tsumoto, K., Shiroishi, M., Yutani, K., and Kumagai, I. (2000) Thermodynamic consequences of grafting enhanced affinity toward the mutated antigen onto an antibody. The case of anti-lysozyme antibody, HyHEL-10. *J. Biol. Chem. 275*, 12813–12820.

43. Murphy, K. P., Freire, E., and Paterson, Y. (1995) Configurational effects in antibody-antigen interactions studied by microcalorimetry. *Proteins 21*, 83–90.

44. Sinha, N., and Smith-Gill, S. J. (2005) Molecular dynamics simulation of a high-affinity antibody-protein complex: the binding site is a mosaic of locally flexible and preorganized rigid regions. *Cell Biochem. Biophys. 43*, 253–273.